P4.6

NUMERICAL SIMULATION OF ROSSBY WAVE BREAKING AND BLOCKING FORMATION USING A SIMPLE BAROTROPIC MODEL

H. L. Tanaka (FRSGC)
Institute of Geoscience, University of Tsukuba
Tsukuba, 305-8571, Japan

1. INTRODUCTION

Recently, a Rossby wave breaking draws more attention in conjunction with an onset of blocking in the troposphere. According to a model simulation by Tanaka (1998), a blocking formation is induced by a breaking Rossby wave which is characterized by an overturning of high and low potential vorticity centers. Once a blocking is formed, the blocking itself then causes further break down of subsequent travelling Rossby waves. In our model, travelling Rossby waves grow exponentially by means of parameterized baroclinic instability, so the waves must break down somewhere. A Rossby wave, which grows critical in amplitude, breaks down when it moves over a topographically induced stationary ridge.

In this blocking theory, the Rossby wave breaking appears to play the key role both for the formation and maintenance of blocking. Therefore, it is important to understand the mechanism and criterion of the Rossby wave breaking in more detail for the study and prediction of blocking formation.

Rossby wave breaking was discussed as an analogy of gravity wave breaking (e.g., McIntyre and Palmer 1983; Fritts 1984; Tanaka and Watarai 1999). Figure 1 schematically compares gravity wave breaking in the vertical section and Rossby wave breaking in the meridional section. When the isentropic surface overturns wrapping up the contours, negative vertical gradient of potential temperature appears as indicated in the figure. The convective instability is the principal mechanism for gravity wave breaking which eliminate the instability through the convective mixing. For the Rossby wave, the dynamical analogy is illustrated with potential vorticity (PV) contours in the meridional plane (see Garcia 1991). When the high and low PV centers roll up to exhibit surf zone structure, negative meridional gradient of potential vorticity appears as indicated in the figure, this being the necessary condition for barotropic-baroclinic instability of the flow.

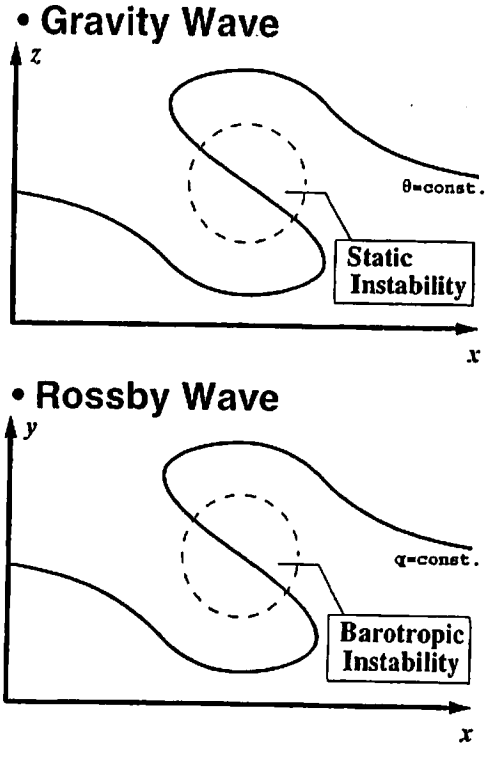

Fig. 1. Schematic illustrations of gravity wave breaking in the vertical section (upper) and Rossby wave breaking in the meridional section (lower).

Although the analogy of Rossby wave breaking is perfectly clear, the theoretical basis of Rossby wave breaking is not well established. For instance, laboratory and field observations indicate that inertial gravity wave breaking leads to the generation of three-dimensional turbulence, whereas the Rossby wave breaking may be treated within the framework of two-dimensional turbulence. The break down of the Rossby wave would produce even larger coherent vortices through the inverse energy cascade. Namely, breaking synoptic-scale waves may result in excitation of planetary waves, which may be a great contrast with the 3-D turbulence. A splitting jet and zonal-

ization may be the realization of such a Rossby wave breaking. Further study is desirable to understand the Rossby wave breaking to confirm if Garcia's analogy is applicable to the study of the blocking formation.

The purpose of this study is to examine the breaking Rossby waves in the barotropic atmosphere using a simple barotropic model which implements parameterization of baroclinic instability. We examine the nonlinear evolution of the growing Rossby waves and the criterion of the wave breaking in the barotropic atmosphere. The energy flows associated with the Rossby wave breaking are extensively examined in the wavenumber domain.

2. MODEL DESCRIPTION

The model description is detailed in Tanaka (1998), and a brief description is presented here. A system of primitive equations with a spherical coordinate may be reduced to the following standard spectral form after proper diagonalization of linear terms using Hough basis functions:

$$\frac{dw_i}{d\tau} + i\sigma_i w_i = -i\sum_{jk} r_{ijk} w_j w_k + f_i, \qquad (1)$$

where w_i and f_i are the Fourier expansion coefficients of dependent variables and forcing terms, τ the dimensionless time, σ_i the eigenfrequency of the Laplace's tidal equation, and r_{ijk} the nonlinear interaction coefficients. The model is truncated at zonal and meridional wavenumbers at 20, including only barotropic Rossby modes which are symmetric about the equator. Only five physical processes are considered in the model for f_i: 1) baroclinic instability, 2) topographic forcing, 3) biharmonic diffusion, 4) zonal surface stress, and 5) Ekman pumping.

In the spectral domain, total energy is simply the sum of the energy elements E_i defined by:

$$E_i = \frac{1}{2} p_s h_m |w_i|^2, \qquad (2)$$

where the dimensional factors p_s and h_m are the surface pressure of the reference state and the equivalent depth of the atmosphere, respectively.

3. RESULTS OF THE EXPERIMENTS

The model equation (1) is integrated in time, starting from an infinitesimal white noise superimposed on a zonal flow. In order to isolate the exponential amplification of unstable modes, the baroclinic instability is imposed in this study only at the zonal wavenumber 6. In this experiment, topography is excluded.

Figure 2 illustrates the time evolution of the total energy for the zonal wavenumber 6 and the zonal motions. The energy level of the initial white noise is of the order of 10 J m^{-2}. After an initial adjustment, the energy level starts to increase exponentially for days from 25 to 50 as expected from the linear theory of instability. The exponential growth, however, must terminate when the wave amplitude becomes finite so that the nonlinear wave-wave interactions become comparable to the linear terms in (1). This may be the stage of wave saturation. The eddy energy is equilibrated at 2×10^5 J m^{-2}. The zonal barotropic energy is approximately constant at 1×10^6 J m^{-2}. It is interesting to note that the eddy energy reaches its equilibrium when the energy level becomes 20% of the zonal barotropic energy.

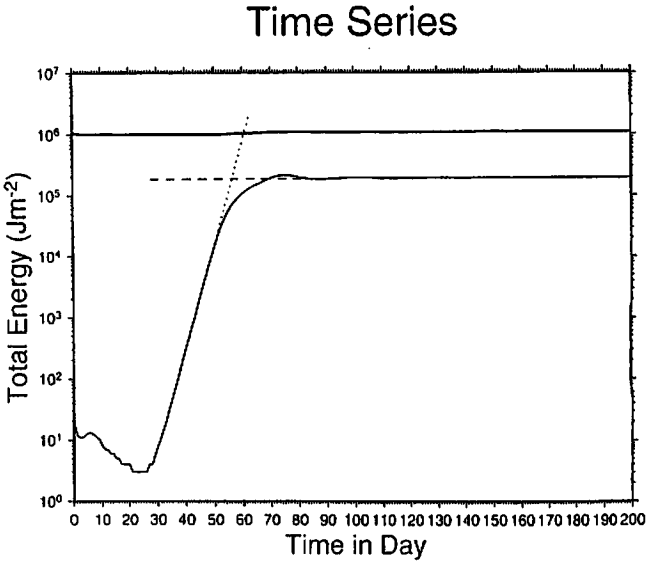

Fig. 2. Time series of total energy in the zonal (thick solid line) and eddy (thin solid line) components during the first 200 days. The crossing of dotted and dashed line represents the saturation point.

Figure 3 illustrates the distribution of geopotential height and its forcing by the parameterized baroclinic instability when the wave reaches finite amplitudes. A rotating wavenumber 6 emerges from infinitesimal noise in mid-latitudes. The height forcing is in phase with the height wave to amplify the wave as expected. The trough axis tilts from northwest to southeast at the northern flank of the westerly jet, whereas it tilts from southwest to northeast at the southern flank. The forcing pattern is consistent with observation in that the eddy momentum

flux converges to mid-latitudes accelerating the westerly jet. The characteristic structure comes from that of the unstable Charney mode anticipated from baroclinic instability theory.

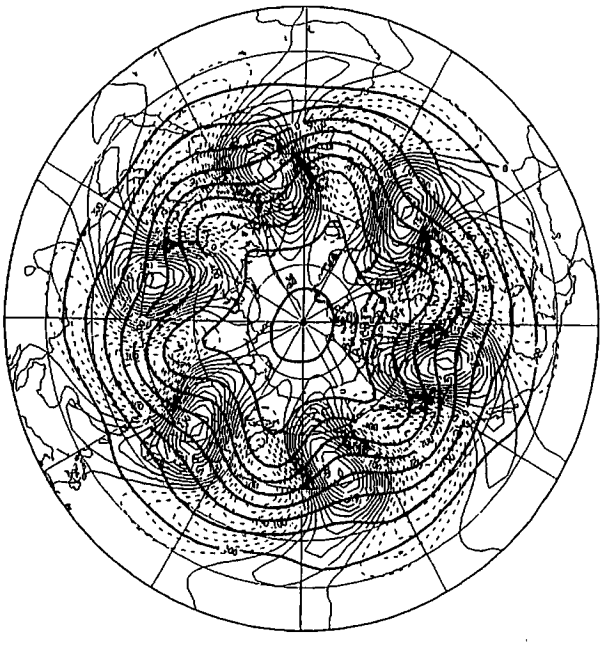

Fig. 3. Geopotential height and the forcing at the saturation point, excited by the wave-6 model.

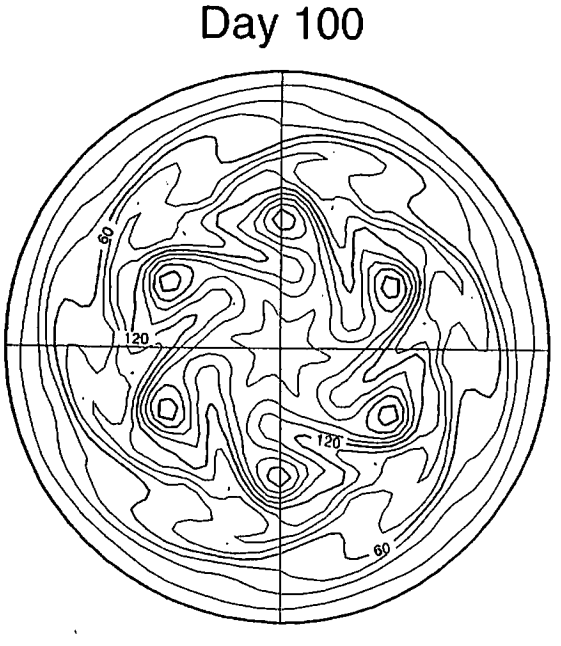

Fig. 4. Potential vorticity (PV) for the day 100. The units are 10^{-10} $m^{-1}s^{-1}$ with the contour interval 15.

Figure 4 illustrates hemispheric distributions of shallow water potential vorticity (PV) for the day 100. A positive and negative vorticity pair appears to rotate anti-clockwise at the saturation point in Fig. 2. The wave is about to break down, indicating a characteristic "surf zone" shape as shown in Fig. 1. Evidently, the meridional gradient of potential vorticity indicates negative area at the surf zone latitudes. Such an area appears on day 48 when the exponential growth of the unstable mode deviates from the theoretical straight line in Fig. 2. In this experiment, however, it is interesting to note that the wave amplitude is saturated, but the wave breaking has not been attained. The surf zone shape of PV attains a steady configuration, and it advects simply from west to east keeping the same structure. The energy supply at n=6 is balanced with energy transfer to zonal flow and to its harmonics of n=12 and 18 by weak nonlinear interactions.

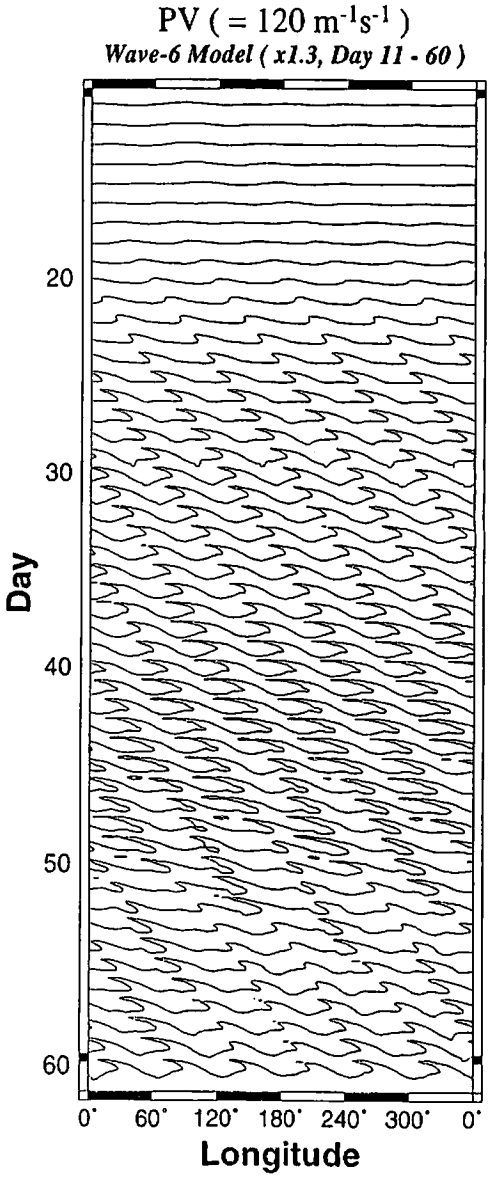

Fig. 5. Schematic illustration of breaking Rossby waves expressed by the contours of 120 PV in Fig. 4 as functions of time (day) and longitudes.

In order to break the wave, we intentionally increase the growth rate of the baroclinic instability by 30%. Figure 5 illustrates the breaking Rossby waves expressed by the collection of 120 PV unit contours as functions of longitude and time for days 11 to 60. The wave amplitudes increase as time proceeds, and the meridional gradient of PV turns to be negative around day 20. (We started from larger white noise than before.) The surf zone shapes develop around days 25. The deformation of the 120 PV unit contours increases for days 40 to 50; this is the period when the wave breaking is identified. Some contours are disconnected to produce a filament of PV contours.

Figure 6 illustrates an example of the PV contours for fully breaking Rossby waves. An overturning of high and low PV indicates the characteristics of the onset of blocking. The energy supply at n=6 is balanced now with energy transfer to all waves, producing a power law in its energy spectrum, consistent with the definition of turbulence.

Fig. 6. Potential vorticity (PV) for fully breaking Rossby waves.

4. EXAMPLE OF BLOCKING FORMATION

An example of blocking formation triggered by a breaking Rossby wave is illustrated in Fig. 7 (see Tanaka 1998; Tanaka and Watarai 1999). Here, topography is included in this experiment. In the figure, contours of shallow water PV are plotted with latitude in the ordinate and longitude in the abscissa in descending order, respectively, in order to mimic the progression and breaking of waves in analogy of shallow water system at the shore. The high PV in the polar region is hatched to illustrate the breaking waves at the surf zone. The elongation of trough and ridge axes from northwest to southeast and the anticlockwise overturning of the vortex pair are the major characteristics of Rossby wave breaking induced by baroclinic instability. The result clearly depicts the consequence of Rossby wave breaking and subsequent blocking formation over the North Pacific.

5. SUMMARY AND DISCUSSION

In this study, we conducted a series of numerical experiments of breaking Rossby wave in the barotropic atmosphere using a simple barotropic model which implements parameterization of baroclinic instability. Exponential growth of unstable modes must terminate eventually when the waves become finite amplitude. The nonlinear evolution of amplified Rossby waves is examined by analyzing the potential vorticity (PV) field in order to assess the criterion of the Rossby wave breaking in a barotropic model atmosphere, which may lead to the formation of atmospheric blocking.

For a control run of the wave-6 experiment, growing unstable wavenumber n=6 is saturated when the wave energy attains approximately 20% of zonal energy of the basic flow. The energy supply at n=6 is balanced with energy transfer to zonal flow and to its harmonics of n=12 and 18 by weak nonlinear interactions, maintaining a steady configuration of a surf zone structure. The existence of the negative meridional gradient of PV is not the sufficient condition for the wave breaking in this experiment.

We then attempted to break the waves intentionally by increasing the growth rate of the unstable mode. It is found that the regularity of Rossby wave progression is lost and the overturning of high and low PV centers occurs when the growth rate is increased by 30%. Associated with the Rossby wave breaking, not only the harmonic waves but also all zonal waves are amplified by the fully nonlinear interactions among all waves. It is demonstrated that the transition from the weakly nonlinear regime to fully nonlinear regime in the energy transfer is the key factor for the Rossby wave breaking so that the supplied energy is effectively dissipated by all waves.

Although a blocking can appear without the help of stationary forcing, the interaction between transient and stationary waves provides a favorable

environment for a persistent blocking formation.

Acknowledgments

This research was partly supported by the Frontier Research System for Global Change. The author appreciates technical supports by Mr. Y. Watarai, Ms. K. Oshoshi, and Ms. K. Honda.

References

Charney, J. G. and Stern, M. E. 1962: On the stability of internal baroclinic jet in a rotating atmosphere. *J. Atmos. Sci.*, **19**, 159–172.

Fritts, D. C. 1984: Gravity wave saturation in the middle atmosphere: A review of theory and observation. *Rev. Geophys. Space Phys.*, **22**, 275–308.

Garcia, R. R. 1991: Parameterization of planetary wave breaking in the middle atmosphere. *J. Atmos. Sci.*, **38**, 2187–2197.

McIntyre, M. E. and Palmer, T. H. 1983: Breaking planetary waves in the stratosphere. *Nature*, **305**, 593–600.

Simmons, A. J., and Hoskins, B. J. 1976: Baroclinic Instability on the sphere: Normal modes of the Primitive and Quasi-geostrophic equations. *J. Atmos. Sci.*, **33**, 1454–1477.

Tanaka, H.L. 1998: Numerical simulation of a life-cycle of atmospheric blocking and the analysis of potential vorticity using a simple barotropic model. *J. Meteor. Soc. Japan*, **76**, 983–1008.

Tanaka, H.L. and Y. Watarai 1999: Breaking Rossby waves in the barotropic atmosphere with parameterized baroclinic instability *Tellus*, **51A**, 552–573.

Fig. 7. A blocking formation triggerred by breaking Rossby waves, drafted for the PV distribution in the barotropic model atmosphere. The high PV in polar region exceeding the value of 120 is hatched.